# Thermally activated motion of pyramidal dislocations through Peierls barriers in zinc single crystals

I. V. Gektina, F. F. Lavrent'ev, and V. D. Natsik

*Physicotechnical Institute of Low Temperatures, Ukrainian Academy of Sciences*
(Submitted 14 May 1980)
Zh. Eksp. Teor. Fiz. **79**, 1927–1935 (November 1980)

The kinetics of the thermally activated motion of screw pyramidal dislocations in zinc crystals is investigated in the temperature range 4.2–295 °K. It is shown that the dislocation path length depends linearly on the loading duration; a lag time $t_i$ is observed. The effect of the stress $\tau$ and temperature $T$ on the dislocation velocity is studied. It is shown that the motion of the dislocation is determined over the entire $\tau$ and $T$ interval by the surmounting of the Peierls barriers. Estimates are obtained for the Peierls stress $\tau_P = 780$ gf/mm$^2$ and the energy of a single kink $V_0 = 0.17$ eV.

PACS numbers: 61.70.Le

## 1. INTRODUCTION

Displacement of a dislocation along crystallographic direction, as is well known, is accompanied by periodic changes in its potential energy; the corresponding potential hill pattern is referred to as Peierls hills. The height of Peierls barriers depends on the type of crystal structure and the kind of crystallographic plane in which the dislocation moves. When the barriers are sufficiently high, they are one of the primary factors determining the mobility of individual dislocations, and consequently also the plastic-deformation kinetics of the entire crystal. Therefore study of the Peierls hills structure and the physical processes promoting passage of the dislocations through the barriers is one of the important problems of dislocation physics.

According to current ideas, the Peierls barriers limit dislocation mobility in crystals with covalent bonding (most semiconductors) and in metals with bcc lattice structure.[1] We should point out that only for some semiconductors (germanium, silicon) are these assumptions based on results of direct observation of the mobility of individual dislocations. In the remaining cases, the success of the Peierls model is based on indirect data obtained from study of Bordoni peaks in the temperature dependence of the internal friction or from an analysis of the macroscopic characteristics of plastic deformation. There is also a large amount of direct and indirect data to indicate that the motion of dislocations in planes with low crystallographic indices in fcc metals and in basal planes of hcp metals is not associated with overcoming appreciably high Peierls barriers. As regards the $\{11\bar{2}2\}\langle 11\bar{2}3\rangle$ pyramidal slip planes in hcp metals, there are grounds for assuming that the Peierls barrier in such metals has an appreciable height.[2] However, up to the present time little direct experimental data confirming this viewpoint has been obtained.

Moreover, in the study of the Peierls mechanism of dislocation deceleration, hcp metals have a number of advantages over semiconductor crystals. It is enough to mention only two of these advantages: firstly, owing to the high plasticity of hcp metals, the mobility curves can be obtained over broader stress intervals than in brittle semiconductors; secondly, pyramidal dislocations in these metals remain mobile over the entire range of temperatures available in the study—from helium temperature to room temperature and above—while in semiconductors, motion of dislocations can be observed only at high temperatures. The importance of the advantages mentioned is due to the fact that only comprehensive data on the dependence of mobility on stress and temperature, over a wide range of these parameters, allows us to reliably establish not only the Peierls hill structure but also the relative role of physical processes promoting the passage of dislocations through the barriers (especially the role of thermal fluctuations).

The laws of plastic deformation and dislocation motion in the $\{11\bar{2}2\}\langle 11\bar{2}3\rangle$ slip system in zinc have been previously studied in a number of papers.[3–9] In experiments on dislocation mobility,[3,4] strain hardening,[7,8] and ultrasound absorption[7–9] it was shown that thermally activated motion of pyramidal dislocations is characterized by the following parameters: activation energy 0.1–0.2 eV, and activation volume $(2-30)b^3$. Such small values of the activation parameters were evidence that pyramidal dislocation motion in Zn is controlled by the surmounting of the peierls barriers.[4,7–9] However, it was not possible to draw final conclusions since systematic and methodologically correct measurements over a sufficiently broad range of temperatures and shear stresses were lacking. Moreover, the major part of the experimental investigations was carried out even before a sufficiently rigorous theory of dislocation motion through the Peierls barriers was established, which made interpretation of the experimental data difficult.

Subsequent theoretical analysis of thermally activated motion of dislocations in a Peierls potential hill pattern was carried out by Petukhov and Pokrovskii.[10] The existence of such a theory and also the improvement in experimental investigation techniques for individual dislocation mobility in recent years have made it possible to approach the problem of identification of the mechanisms of pyramidal dislocation mobility at a qualitatively new level.

The task of our work was to study dislocation mobility in the $\{11\bar{2}2\}\langle 11\bar{2}3\rangle$ slip system over a broader temperature interval and with a more accurate technique than

 0038-5646/80/110973-05$02.40  

previously,[3-6] and to compare the experimental data with the theoretical results.[10]

## 2. EXPERIMENTAL TECHNIQUE

We used Zn single crystals of 99.997% purity, grown according to the procedure described by Vladimirov *etal.*[11]; the basal (0001) plane was parallel to the growth axis. The crystals were cut by the electric spark technique into blocks which were annealed for 50 hours at 380°C and then cleaved along the (0001) plane at 77°K into prismatic samples with dimensions 3×3×8 mm and 4×4×9 mm. In the samples prepared by such means, the basal dislocation density was $\rho_b = 5 \cdot 10^5$ cm$^{-2}$, the pyramidal dislocation density was $\rho_p \approx (3-4) \cdot 10^3$ cm$^{-2}$, and small-angle faces were absent.

The samples were deformed by compression along the $[11\bar{2}0]$ axis at constant stress. The magnitudes of the shear stress $\tau$ in the $\{11\bar{2}2\}\langle 11\bar{2}3\rangle$ slip system were varied from 120 to 740 gf/mm$^2$; the starting stress for onset of dislocation motion in these crystals is equal to 110 gf/mm$^2$.[12] The loading time varied from 0.15 to $1.8 \cdot 10^4$ seconds.

Freshly formed dislocations were introduced by scoring scratches on the (0001) plane in the $[11\bar{2}0]$ direction. After loading, the displacements of the screw components of the pyramidal dislocations were measured. The dislocation density and path lengths (lengths of the slip line) were determined by selective chemical etching.[5,13]

The investigation was carried out at 4.2, 77, 144, 220, and 295°K. At each temperature, the dislocation path length $l$ was plotted vs the loading time $t$ for several values of the shear stress (the kinetic curves). The path lengths varied from 30 to 4000 $\mu$. Each point on the $l(t)$ graph corresponds to measurement of the path lengths of 30–80 dislocations.

## 3. EXPERIMENTAL RESULTS

On Fig. 1 we present as an example the kinetic curves for different shear stresses obtained at 144°K. The $l(t)$ curves obtained at other temperatures are qualitatively similar to these. The characteristics of the curves are as follows:

1) The $l(t)$ curves are linear for average path lengths up to $l \lesssim 2 \cdot 10^3$ $\mu$ (in this case, many dislocations traverse a path of $l \approx (3-4) \cdot 10^3$ $\mu$; with further increase in $\bar{l}$, deviation from linearity is observed in several $l(t)$ curves. The reasons for the deviation of the kinetic curves from linearity at $l > 2 \cdot 10^3 \mu$ was not specially studied.

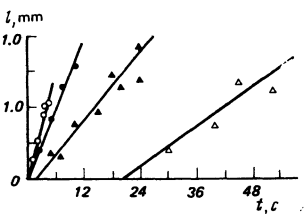


FIG. 1. Average dislocation path length vs. duration of loading at 144°K: △ – $\tau$ = 140 gf/mm$^2$, ▲ – 160, ● – 180, ○ – 200.

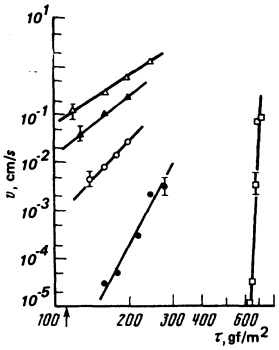


FIG. 2. Dislocation velocity vs. shear stress at different temperatures: △ – $T$ = 295 K, ▲ – 220, ○ – 144, ● – 77, □ – 4.2. The value of $\tau_{st}$ is indicated by the arrow.

2) All the kinetic curves intercept a segment on the $t$ axis, the so-called lag time[1)] $t_i$; in the temperature and shear stress range studied, the lag time decreases with an increase in $T$ and (or) $\tau$; the range over which $t_i$ varies is from $10^{-1}$ to $5 \cdot 10^3$ seconds.

The linearity of the $l(t)$ curves obtained shows that in the experiments carried out at constant stress, the dislocation velocity [defined as the slope of the linear portion of $l(t)$] is constant over a wide range of path lengths. The plots of dislocation velocity vs. shear stress for temperatures of 4.2–295 °K are presented in Fig. 2 on a logarithmic scale. On lowering the temperature, the graphs of $v(\tau)$ are shifted toward the higher stress region. In the literature it is customary to plot the mobility curves in the coordinates $v \sim \tau^m$. As is evident from Fig. 2, in our case the exponent $m$ in the functional relationship $v \sim \tau^m$ is increased as the temperature is lowered—from 3 to 295°K at 87 at 4.2°K.

On Fig. 3 we show the plots of $v$ vs $1/T$ for different shear stress levels. It is evident that the dislocation motion is thermally activated and may be described by an Arrhenius relationship. Extrapolation of the obtained $v(1/T)$ curves to $1/T = 0$ makes it possible to determine the pre-exponential factor $v_0$ as a function of stress. It was shown that $v_0 \sim \tau^{1.3}$ for stresses from 120 to 300 gf/mm$^2$. From the reduction of the experimental data we obtained plots of the thermal activation parameters

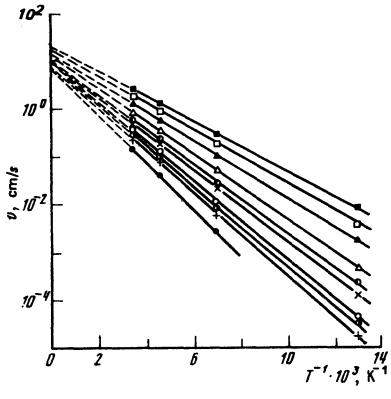


FIG. 3. Dislocation velocity vs. $1/T$ for different shear stress: ● – $\tau$ = 130 gf/m$^2$, + – 150, ◑ – 160, ○ – 170, × – 190, ◑ – 200, △ – 220, ▲ – 250, □ – 280, ■ – 300.

vs. stress in the range 120–740 gf/mm$^2$; the activation energy varies from 0.01 to 0.1 eV, and the activation volume from $5 \cdot 10^{-22}$ to $7 \cdot 10^{-21}$ cm$^3$.

## 4. COMPARISON OF EXPERIMENTAL DATA WITH THEORY

The low values of the activation energy and activation volume provide a basis for assuming that the motion of pyramidal dislocations in Zn is controlled by the decelerating effect of the Peierls hills. Therefore we must discuss in detail the data obtained from the point of view of the theory of thermally activated surmounting of Peierls barriers.[10]

The motion of dislocations in the Peierls hills at stresses $\tau < \tau_p$ occurs by means of thermal-fluctuation formation and further broadening of double kinks. The average dislocation velocity $v$ is related to the probability $w$ of developing a kink of critical dimensions as $v \sim w^{1/2}$. In the classical limit, the expression for the dislocation velocity takes the form

$$v = v_0 \exp\left[-H(\tau)/kT\right]. \tag{1}$$

The explicit form of the activation energy $H(\tau)$ and of the pre-exponential factor $v_0$ was obtained by Petukhov and Pokrovskii[10] for two limiting values of the stress, $\tau \ll \tau_p$ and $\tau \to \tau_p$. We should point out that $v_0$ also depends on $\tau$ and $T$; however, this dependence is weak (a power law relationship with a small exponent) and taking it into account changes the overall result only slightly. Subsequently, we will neglect this dependence in treatment of the experimental data, a procedure acceptable if we consider the significant spread in the experimental points.

In the indicated limiting cases, $H(\tau)$ is determined by the expressions

$$H(\tau) = V_0 - b^2 l_0 \tau \ln(\tau_0/\tau), \quad \tau \ll \tau_P; \tag{2}$$

$$H(\tau) = H_0(1-\tau/\tau_P)^{3/4}, \quad \tau_P - \tau \ll \tau_P. \tag{3}$$

The constants $V_0$, $l_0$, $\tau_0$, and $H_0$ in these equations depend on the magnitude of the Burgers vector $b$, on the tension coefficient of the dislocation $C$, and on the parameters of the Peierls potential $U_P(y)$ ($y$ is the coordinate along the dislocation motion). The parameter $V_0$ represents the energy of a single kink; this energy was computed by Guyot and Dorn[15] for certain specific forms of $U_P(y)$. The expressions for the remaining constants have the form

$$l_0 = \frac{a}{2b}\left(\frac{C}{U_P''}\right)^{1/2}, \quad \tau_0 = \frac{a}{2b}U_P'', \qquad H_0 = 2^{1/4} \cdot 2^{4}/_{5} C^{1/2}(b\tau_P)^{3/4}(|U_P'''|)^{-1/4}. \tag{4}$$

Here

$$U_P'' = \left[\frac{\partial^2}{\partial y^2}U_P(y)\right]_{y=0}$$

is the value of the second derivative of the function $U_P(y)$ at the minimum point;

$$U_P''' = \left[\frac{\partial^3}{\partial y^3}U_P(y)\right]_{y=y_0}$$

is the value of the third derivative at the inflection point $y_0$, where the first derivative $\partial U_P(y)/\partial y$ reaches a maximum; the Peierls stress $\tau_P$ is defined by the relationship

$$b\tau_P = \left[\frac{\partial}{\partial y}U_P(y)\right]_{y=y_0};$$

$a$ is the period of the function $U_P(y)$.

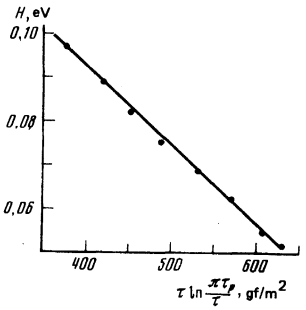


FIG. 4. $H[\tau \ln(\pi\tau_P/\tau)]$ curve for the low-stress region, $\tau_P = 780$ gf/mm$^2$.

From Eqs. (2) and (3) it is easy to obtain the expressions describing the activation volume $\gamma(\tau) = -\partial H(\tau)/\partial\tau$:

$$\gamma(\tau) = b^2 l_0\left(\ln\frac{\pi\tau_P}{\tau} - 1\right), \quad \tau \ll \tau_P, \tag{5}$$

$$\gamma(\tau) = \gamma_0\left(1 - \frac{\tau}{\tau_P}\right)^{1/4}, \quad \tau_P - \tau \ll \tau_P, \tag{6}$$

$$\gamma_0 = 2^{3/4} \cdot 3 b^{3/4} C^{1/4} \tau_P^{3/4} (|U_P'''|)^{-1/4}.$$

The values of the constants in the theory may be related to the measured parameters of the crystal for a sinusoidal Peierls hill pattern

$$U_P(y) = \frac{1}{2}U_0\left(1 - \cos\frac{2\pi y}{a}\right),$$

by using the relationship $C \approx Gb^2$, where $G$ is the shear modulus in the slip direction;

$$V_0 = Gb^3(2a/\pi b)^{1/2}(\tau_P/G^{1/2}), \quad l_0 = b\pi^{1/2}(a/2b)^{1/2}((G/\tau_P)^{1/2},$$
$$\tau_0 = \pi\tau_P, \quad \tau_P = \frac{\pi U_0}{ab}, \tag{7}$$
$$H_0 = \frac{2}{\pi^{1/2}}\left(\frac{a}{b}\right)^{1/2}\left(\frac{\tau_P}{G}\right)^{1/2} Gb^3, \quad \gamma_0 = \frac{5}{2\pi^{1/2}}\left(\frac{a}{b}\right)^{1/2}\left(\frac{G}{\tau_P}\right)^{1/2} b^3.$$

From Eqs. (2)–(6) it is evident that the activation parameters $H$ and $\gamma$ depend differently on $\tau$ in the high and low stress regions.

Let us analyze the experimental data obtained in the appropriate coordinates. On Fig. 4 and Fig. 5 we present the plots of $H$ vs $\tau \ln(\pi\tau_P/\tau)$ and $\gamma$ vs $\ln(\pi\tau_P/\tau) - 1$ for stresses of 120–300 gf/mm$^2$. In the reduction

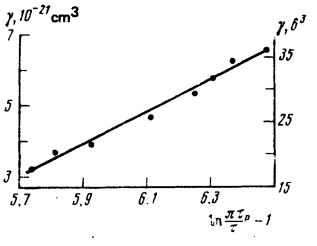


FIG. 5. $\gamma[\ln(\pi\tau_P/\tau) - 1]$ for the low-stress region, $\tau_P = 780$ gf/mm$^2$.

the experimental data we used, for the parameter $\tau_P$ a set of stress values from 750 to 1200 gf/mm$^2$. It turned out that the experimental data were best linearized in the coordinates corresponding to Eqs. (2), (3), (6), for $\tau_P = 780$ gf/mm$^2$. It is evident that the curves on Figs. 4 and 5 are linear; the slopes are close to $17b^3$ for $H$ and $23b^3$ for $\gamma$. Extrapolation of the curves of $H$ vs $\tau \ln(\pi\tau_P/\tau)$ to the zero value of the function $\tau \ln(\pi\tau_P/\tau)$ gives $V_0 = 0.17$ eV. An estimate of the parameters $b^2 l_0$ and $V_0$ from Eq. (7) gives $b^2 l_0 = 5b^3$ and $V_0 = 0.10$ eV, if we take for the crystal parameters entering into Eq. (7) the values $G = 2.97 \cdot 10^{11}$ dyne/cm$^2$, $a = 2.6 \cdot 10^{-8}$ cm, and $b = 5.65 \cdot 10^{-8}$ cm.

On Fig. 6 we give plots of $\gamma$ vs $(1 - \tau/\tau_P)^{1/4}$ for stresses above 650 gf/mm$^2$. The experimental points fit well a straight line at $\tau \geq 680$ gm-f/mm$^2$; the value $\gamma_0 = 8b^3$ determined from this plot agrees well with the $\gamma_0 = 9b^3$ calculated from Eq. (7).

Thus, the experimental data obtained on mobility of pyramidal dislocations in the temperature range 4.2–295 °K for low and high stress are satisfactorily described by the theory of dislocation motion in the Peierls hills.[10] In particular, the experiment confirms the curves obtained theoretically[10] for the stress dependence of the activation parameters; we note that the form of these dependences is not associated with a specific form of the Peierls function $U_P(y)$. The numerical values of the constants $V_0$ and $b^2 l_0$, calculated assuming a sinusoidal form for the Peierls hills pattern, differ from those found from analysis of the experimental data by several-fold; apparently, such a shape for the hill pattern is not too good an approximation in the calculation of the quantities $U'_P$ and $U''_P$ in Eq. (4). As $\tau \to \tau_P$, this approximation gives better agreement between the calculated and observed values of the parameter $\gamma_0$, which is determined only the the third derivative $U'''_P$.

On the basis of the analysis performed, we can state that the mechanism controlling the mobility of pyramidal dislocations in Zn is the surmounting the Peierls hills.

We should point out that the results of our work differ substantially from the results of Blish and Vreeland,[4] who studied the mobility of pyramidal dislocations in Zn in the temperature range 77–323 °K. A complex functional dependence for $v(T)$ was obtained by them[4] at constant $\tau$: the dislocation velocity first grows as the temperature increases, while at $T > 200$ °K it decreases. The shape of the $v(T)$ curve observed is connected with a change in the mechanism controlling the velocity, the double kink mechanism at 77–110 °K, and cross-glide above 200 °K. However, as is shown in our work (see Fig. 2) the pyramidal-dislocation velocity is a monotonic function of temperature for any shear stress and is controlled over the entire range of $T$ and $\tau$ by a single mechanism—the surmounting the Peierls barriers.

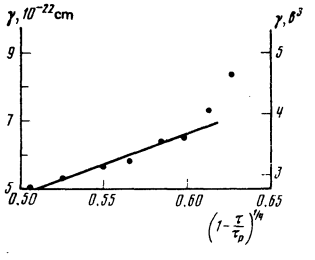


FIG. 6. $\gamma[(1 - \tau/\tau_P)^{1/4}]$ for the high-stress region.

We should point out that cross-glide of screw components of pyramidal dislocations was observed in our experiments, as previously.[4,16] With increase in temperature, the slip bands are appreciably broadened; this is due to activation of the double cross-glide.[17] The agreement between the activation parameters obtained in this work and those obtained previously[17] is apparently evidence that the double cross-glide of the screw components of the pyramidal dislocations is determined by the same barriers which control the motion, i.e., the Peierls hills.

Substantial differences between our experimental data and that of Ref. 4 may probably be explained by the fact that in Ref. 4 the measurements were performed with fixed loading times on slip lines arising from random sources. It is clear that neglect of the nonlinearity of the $l(t)$ curve for long path lengths and lag times $t_l$, which reach significant values, leads to substantial errors in the determination of dislocation velocity and in the dependence of the velocity on shear stress and temperature.

In this work we studied the motion of dislocations in the Peierls hills at helium temperatures; therefore we should discuss in particular the possibility of observing quantum effects on such motion.[10] Theory[10] predicts that as $\tau \to \tau_P$ the motion of dislocations takes on a quantum character at temperatures on the order of

$$T_0(\tau) \approx 10^{-1} \left(\frac{\tau_P}{G}\right)^{1/2} \left(1 - \frac{\tau}{\tau_P}\right)^{1/4} T_D, \qquad (8)$$

where $T_D$ is the Debye temperature. In our case, the temperature $T_0 \sim 0.3$ °K for $\tau_P - \tau \sim 0.1\tau_P$; therefore, at $T = 4.2$ °K the dislocation motion should still have a completely thermal activation character—which is confirmed in the experiment. At present, it has become feasible to study dislocation motion at temperatures below 1 °K.[18,19] This encourages us to hope that the theoretical results involving this point will also be tested in the near future.

The authors thank S. V. Lubenets, A. I. Landau, and V. I. Dotsenko for valuable comments and helpful discussion of the research results.

[1)] The lag time for static loading was observed earlier by Lubenets and Ostapchuk[14] in KCl crystals.

[1] I. E. Bondarenko and V. I. Nikitenko, in: Problemy prochnosti i plastichnosti tverdykh tel (Problems in strength and Plasticity of Solids), Nauka, Lenigrad, 1979, p. 244.
[2] H. S. Rosenbaum, in: Deformation Twinning (R. E. Reed-Hill, J. P. Hirth, and H. C. Rogers, eds.), Gordon and Breach, New York, 1963, p. 43.

[3]K. H. Adams, R. C. Blish, II, and T. Vreeland, Jr., Mat. Sci. Eng. 2, 201, (1967).
[4]R. C. Blish, II, and T. Vreeland, Jr., J. Appl. Phys. 40, 884 (1969).
[5]F. F. Lavrent'ev and O. P. Salita, Fiz. Metal. Metalloved. 23, 548 (1967).
[6]F. F. Lavrentev, O. P. Salita, and V. L. Vladimirova, Phys. Stat. Sol. 29, 569 (1968).
[7]Ya. M. Soifer and V. G. Shteinberg, Phys. Stat. Solidi (A) 6, 409 (1971).
[8]Ya. M. Soifer and V. G. Shteinberg, Phys. Stat. Solidi (A) 10, K113 (1972).
[9]M. Mongy, S. A. Z. Mahmoud, S. Saleh, and R. Kamel, Acustica 43, 333 (1979).
[10]B. V. Petukhov and V. L. Pokrovskii, Zh. Éksp. Teor. Fiz. 63, 634 (1972). [Sov. Phys. JETP 36, 336 (1972)].
[11]V. L. Vladimirova, F. F. Lavrent'ev, Yu. A. Pokhil, and S. V. Sokol'skii, Ukr. Fiz. Zh. (Russ. Ed.) 18, 959 (1973).
[12]I. V. Gektina and F. F. Lavrent'ev, Fiz. Met. Metalloved. 41, 1118 (1976).
[13]R. G. Brandt, K. H. Adams, and T. Vreeland, Jr., J. Appl. Phys. 34, 587 (1963).
[14]S. V. Lubenets and E. I. Ostapchuk, Fiz. Tverd Tela (Leningrad) 17, 3416 (1975) [Sov. Phys. Solid State 17, 2235 (1975)].
[15]P. Guyot and J. E. Dorn, Canad. J. Phys. 45, 983 (1967). (Russ. Transl. in: Aktual'nye voprosy teorii dislokatsii (Current Topics in Dislocation Theory), Mir, 1968, p. 270).
[16]I. V. Gektina, F. F. Lavrent'ev, and V. I. Startsev, Fiz. Met. Metalloved. 37, 1275 (1974).
[17]F. F. Lavrent'ev and O. P. Salita, in: Fizicheskie protessy plasticheskoi deformatisii pri nizkikh temperaturakh (Physical Process of Plastic Deformation at Low Temperatures), Naukova Dumka, Kiev, 1974, p. 100.
[18]I. N. Kuz'menko, T. A. Parkhomenko, and V. V. Pustovalov, Fiz. Nizk. Temp. 4, 1340 (1978) [Sov. J. Low Temp. Physics 4, 632 (1978)].
[19]E. Kuramoto, F. Iida, T. Hashimoto, and S. Takeuchi, Scripta Met. 8, 367 (1976).

Translated by Cathy Flick

# Increase of resistance of bismuth deformed at 80 K when the temperature is lowered to the helium region

I. L. Bronevoĭ

*Institute of Physics Problems, USSR Academy of Sciences*
(Submitted 19 May 1980)
Zh. Eksp. Teor. Fiz. **79**, 1936–1941 (November 1980)

The temperature dependence of the resistivity $\rho(T)$ of bismuth is measured in the range $0.4 < T < 8$K at various values of the residual resistivity obtained by deforming the sample at 80 K (the value of $\rho$ in the helium region increased upon deformation by 300–900 times). With increasing deformation, the $\rho(T)$ plot first becomes steeper and then, at low temperature, $d\rho/dT$ begins to decrease and reverses sign. In the low temperature limit, $\rho(T)-\rho(0) \sim -T^n\rho(0)^m$, where $n = 0.5 \pm 0.15$ and $0.8 < m < 1.1$. A comparison is made with theory of Al'tshuler and Aronov [Sov. Phys. JETP **50**, 968 (1979) and JETP Lett. **27**, 662 (1978)], according to which $n = 0.5$.

PACS numbers: 72.15.Eb

Sharvin and the author[1] observed an increase of the resistivity $\rho(T)$ when the temperature of a bismuth wire, strongly deformed at 80 K, was lowered to the liquid-helium region. Since the appearance of the anomaly was not due to introduction of magnetic impurities, it can be assumed that it was not caused by the Kondo effect.

The observed effect, as noted by Al'tshuler and Aronov, was of the same order as estimated by their theory (see Ref. 2 and the earlier Ref. 3), which deals with the effect of the interference between the electrons and of their elastic scattering by lattice inhomogeneities According to their theory[2,3] the contribution of this mechanism to the $\rho(T)$ dependence for an isotropic model takes at $kT \ll \hbar/\tau$ the form

$$[\rho(T)-\rho(0)]/\rho(0) = C(T\tau)^{1/2}(p_F l)^{-2}, \quad (1)$$

where $l$ and $\tau$ are the electron mean free path length and time, $p_F$ is the Fermi momentum, and the constant $C$ is negative for a repulsion interaction between the electrons.

By deforming bismuth at low temperatures it is possible to obtain values of $\rho(0)$ large enough to satisfy at helium temperature the condition $kT \ll \hbar/\tau$ (the value obtained in Ref. 1 for a deformed wire was $\rho = 1.9 \times 10^{-3}$ Ω-cm, leading to the estimate $\hbar/k\tau = 190$ K; for the data on the electron spectrum of bismuth see, e.g., Ref. 4).

For a more detailed study of the effect and for a comparison of the results with the theory of Refs. 2 and 3, we have measured $\rho(T)$ in a larger temperature interval $0.4 < T < 8$ at various degrees of plastic deformation.

## EXPERIMENT

In the initial form, the samples were bismuth single crystals in the form of rectangular parallelepipeds measuring $0.25 \times 0.37 \times 18$ mm, growth from the melt in a dismountable mold of construction similar to that described in Ref. 5. The parts of the mold were made of glass and stainless steel. Prior to the casting the mold was coated with a thin layer of vacuum grease and

 0038-5646/80/110977-04$02.40  